Received: 18 January 2022 | Revised: 9 March 2022 | Accepted: 24 March 2022

DOI: 10.1002/mp.15644

RESEARCH ARTICLE

MEDICAL PHYSICS

Range uncertainty reductions in proton therapy may lead to the feasibility of novel beam arrangements which improve organ-at-risk sparing

Sebastian Tattenberg[1,2] | **Thomas M. Madden**[2] | **Thomas Bortfeld**[2] | **Katia Parodi**[1] | **Joost Verburg**[2]

[1]Department of Medical Physics, Faculty of Physics, Ludwig-Maximilians-Universität München, Garching, Germany

[2]Division of Radiation Biophysics, Department of Radiation Oncology, Massachusetts General Hospital and Harvard Medical School, Boston, Massachusetts, USA

Correspondence
Sebastian Tattenberg, Department of Medical Physics, Faculty of Physics, Ludwig-Maximilians-Universität München, Garching, Germany.
Email: stattenberg@mgh.harvard.edu

Funding information
US Federal Income, Grant/Award Number: C06-CA059267; HHS | NIH | National Cancer Institute (NCI), Grant/Award Number: R01-CA229178

Abstract

Purpose: In proton therapy, dose distributions are currently often conformed to organs at risk (OARs) using the less sharp dose fall-off at the lateral beam edge to reduce the effects of uncertainties in the in vivo proton range. However, range uncertainty reductions may make greater use of the sharper dose fall-off at the distal beam edge feasible, potentially improving OAR sparing. We quantified the benefits of such novel beam arrangements.

Methods: For each of 10 brain or skull base cases, five treatment plans robust to 2 mm setup and 0%–4% range uncertainty were created for the traditional clinical beam arrangement and a novel beam arrangement making greater use of the distal beam edge to conform the dose distribution to the brainstem. Metrics including the brainstem normal tissue complication probability (NTCP) with the endpoint of necrosis were determined for all plans and all setup and range uncertainty scenarios.

Results: For the traditional beam arrangement, reducing the range uncertainty from the current level of approximately 4% to a potentially achievable level of 1% reduced the brainstem NTCP by up to 0.9 percentage points in the nominal and up to 1.5 percentage points in the worst-case scenario. Switching to the novel beam arrangement at 1% range uncertainty improved these values by a factor of 2, that is, to 1.8 percentage points and 3.2 percentage points, respectively. The novel beam arrangement achieved a lower brainstem NTCP in all cases starting at a range uncertainty of 2%.

Conclusion: The benefits of novel beam arrangements may be of the same magnitude or even exceed the direct benefits of range uncertainty reductions. Indirect effects may therefore contribute markedly to the benefits of reducing proton range uncertainties.

KEYWORDS
proton therapy, range uncertainty, robust optimization

1 | INTRODUCTION

One of the main motivations behind treating cancer patients with external proton therapy rather than a conventional photon-based treatment is the sharp dose fall-off at the distal proton beam edge, which allows for more conformal dose distributions.[1] However, in practice, uncertainties in the in vivo proton range often

prevent the sharp dose gradient at the distal beam edge from being fully utilized. Such range uncertainties stem from many different sources, including differences in the daily patient setup and inaccuracies in the photon-derived tissue stopping powers relative to water.[2] There are a variety of approaches to address the presence of range uncertainties. The less steep dose fall-off at the lateral beam edge can be used to conform the dose distribution to nearby organs at risk (OARs) instead to reduce the effects of uncertainties in the proton range.[3] Robust treatment planning addresses the issue of range uncertainties by assuring consistent target coverage and/or OAR sparing in a variety of setup and/or range error scenarios.[4,5] However, such approaches generally contribute to an acceptable dose distribution in a wide range of error scenarios at the cost of increased OAR and healthy tissue doses in scenarios of low uncertainty.

Different approaches to reduce range uncertainties in proton therapy are currently being investigated. These approaches can broadly be separated into two different categories: imaging-based methods which aim to reduce the range uncertainties of the treatment planning images, and range monitoring techniques which rely on measurements conducted during or soon after irradiation and which aim to verify the exact position in the patient at which the protons stopped. The former category includes dual-energy computed tomography (DECT), which has been shown to provide more accurate proton stopping power ratios (SPRs) relative to water than conventional single energy spectrum CT scans.[6,7,8] Proton-based CT approaches, which would allow for more direct measurements of tissue stopping powers relative to water, are also under consideration.[9,10,11,12] An early range verification approach which is still being pursued today is based on positron emission tomography (PET) measurements of activated nuclei in the patient shortly after irradiation.[13,14,15,16,17] More recently, projects measuring prompt gamma rays emitted during treatment for real-time range monitoring have also seen development.[18,19,20,21]

The direct dosimetric benefits of proton range uncertainty reductions have been investigated in previous studies, including our own work which quantified these benefits in a set of skull base cases.[22,23,24] However, previous studies focused on OAR dose decreases caused directly by reductions in the range uncertainty, but reducing the range uncertainty may have additional indirect effects on doses to healthy tissues and organs at risk. They may, for example, lead to the feasibility of novel beam arrangements.

This is because delivery techniques making greater use of the steep dose fall-off at the distal beam edge are known to be beneficial in terms of the sparing of nearby OARs. Distal edge tracking (DET), for example, is able to achieve preferential OAR doses by placing Bragg peaks on the target's distal edge.[25] Such techniques are, however, very susceptible to range uncertainties, as additional dose would be "pushed" into the OAR in question in overshoot scenarios.[26,27,28] Treatment plans therefore currently generally make greater use of the less steep dose fall-off at the lateral beam edge to reduce the effects of range uncertainties.[3]

Reductions in the proton range uncertainty could lead to the feasibility of novel beam arrangements which make greater use of the distal beam edge and are therefore able to maintain target coverage while reducing OAR and healthy tissue doses when the range uncertainty is low. To evaluate the full benefit of range uncertainty reductions, indirect benefits such as the effects of such novel beam arrangements therefore also have to be considered. In this study, we investigate the benefits of proton range uncertainty reductions not only in terms of the normal tissue complication probability (NTCP) and healthy tissue dose reductions caused by range uncertainty reductions directly, but also with respect to the benefits of novel beam arrangements which they may render feasible.

2 | METHODS

For every studied case, we created a novel beam arrangement in addition to the traditional clinical one. The novel beam arrangement was chosen so that greater use was made of the sharper dose fall-off at the distal beam edge to conform the dose distribution to the brainstem, which abutted the target in all cases. For each of the two beam arrangements, five treatment plans were created, which were made robust to setup errors of 2 mm as well as range uncertainties of 0%–4%, in increments of 1%. For all treatment plans, OAR metrics such as NTCPs were determined, and the differences in these metrics between different beam arrangements and levels of range uncertainty robustness were used to evaluate the benefits of reducing the range uncertainty, both in terms of the direct effects of range uncertainty reductions as well as with respect to the benefits of novel beam arrangements made feasible by reductions in the range uncertainty.

2.1 | Patient selection and treatment plan creation

This study encompassed treatment plans for 10 skull base and brain cancer patients with targets abutting the brainstem who had received pencil beam scanning (PBS) proton therapy at Massachusetts General Hospital (MGH). All treatment plans included all clinical planning constraints and objectives. The treatment planning system used was our in-house Astroid system, and doses were calculated using the pencil-beam algorithm.[29,30] All treatment plans used the machine

model of the ProTom Radiance 330 system as installed at MGH's recently opened Gordon-Browne Proton Therapy Center. Using a modern machine model was important because the investigated range uncertainty reductions are likely to only be achieved in several years. Using a modern system that is likely optimized in terms of a small lateral penumbra was also considered a fairer comparison than relying on an older system with a natively larger lateral penumbra. For proton energies between 70 MeV and 230 MeV, the spot size in air at isocenter ranged from about 7 mm to about 3.5 mm sigma.

2.2 | Beam angle selection approach

For each of the studied cases, a total of 10 treatment plans were created, five of which made use of the traditional clinical beam arrangement and five of which used the novel beam arrangement. The five treatment plans per beam arrangement were related to the five different levels of range uncertainty robustness, which ranged from 0%–4%, in increments of 1%. The novel beam arrangement used the same number of beams as the traditional clinical beam arrangement, and its beam angles were chosen so that greater use was made of the sharp dose fall-off at the distal beam edge to conform the dose distribution to the brainstem.

Besides greater reliance on the distal beam edge, several additional requirements were placed on the novel beam arrangement:

- **General healthy tissue doses** were required to be lower than or comparable to the traditional clinical beam arrangement to prevent an increase in the risk of long-term healthy tissue damage
- **Doses to OARs other than the brainstem** were likewise required to be comparable to the traditional clinical beam arrangement to assure that the novel beam arrangement did not create an unintended trade-off between the dose to the brainstem and doses to other OARs

During beam angle selection, care was taken with respect to the separation between beam angles to prevent the novel beam arrangement from inadvertently increasing the general healthy tissue volume receiving a high dose. A reduction in the path length of brain exposure was also a consideration. Further deciding factors were often patient-specific and frequently concerned other nearby organs at risk. Particular attention was, for example, paid to the dose delivered to the cochlea and temporal lobes. Depending on the exact target location and size, other common considerations concerned air cavities like the ones in the mastoid region.

The process through which the novel beam arrangement was defined consisted of the following steps:

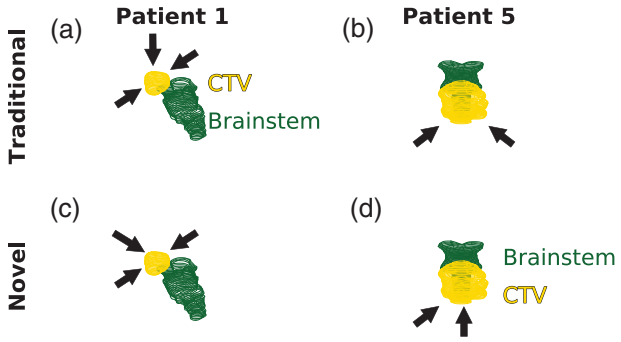

FIGURE 1 The (a,b) traditional clinical and (c,d) novel beam arrangement for patients 1 (left) and 5 (right). Beam angles are indicated by arrows. The yellow and the green structures depicted are the clinical target volume (CTV) and the brainstem, respectively

1. Definition of an (initial) patient-specific novel beam arrangement making greater use of the distal beam edge to conform the dose distribution to the brainstem
2. Fluence optimizations with 4% range uncertainty robustness for both beam arrangements
   a. If an unintended trade-off between the dose to the brainstem and other OARs was observed, the initial novel beam arrangement was adapted, and the optimization was re-run
3. Optimizations for all remaining levels of range uncertainty robustness

The traditional and novel beam arrangements for two patients are shown in Figure 1.

2.3 | Fluence optimizations

The optimization and dose distribution evaluation approaches were in line with our previous work.[24] Fluence optimizations used the Nymph algorithm, a primal-dual infeasible interior point algorithm.[31,32] All optimizations used $\varepsilon = 0.1$ Gy(RBE), meaning that optimizations were completed when the difference between the objective values and the optima were at most 0.1 Gy(RBE). Fluence optimizations required the following inputs:

- **Planning constraints**: We assume that these need to be fulfilled in every scenario, and denote these as $c(x) \leq 0$, where c is a convex vector-valued function;
- **Planning objectives**: are fulfilled as much as possible, with each planning objective f_i being designated a weight ω_i which denotes its relative importance; and
- ***D* matrices**: the matrix D^s for every scenario s; D^s contains matrix elements D_{ij}^s, which denote the dose deposited in voxel i per unit of fluence from proton pencil beam j.

Throughout this work, scenario refers to error scenarios in which setup and/or range errors are applied as

well as to the nominal scenario, which is defined as the scenario in which neither setup nor range errors of any magnitude occur.

Planning constraints used for this work regarded the minimum or minimum mean dose (for target structures) and the maximum or maximum mean dose (for OARs, healthy tissues, and conformality structures). Objective functions included maximize minimum and maximize mean dose (for target structures), minimize maximum and minimize mean dose (for OARs, healthy tissues, and conformality structures), and minimize over-/underdose with respect to a specified bound, which was used to improve target coverage or OAR sparing without the severity of a planning constraint.

Since planning objectives do not have to be fulfilled, an approach to implement planning objectives from different scenarios had to be chosen, and worst-case optimization, which optimizes a single worst-case scenario rather than, for example, considering worst-case scenarios for all objectives separately, was applied[4]:

$$\min_{x\geq 0}\left\{\max_{s\in S}\sum_{i=1}^{k}\omega_i f_i\left(d\left(x;s\right)\right):c\left(x\right)\leq 0\right\} \quad (1)$$

In Equation (1), x is the pencil beam spot weight, s denotes a scenario, f_i is an objective function with weight ω_i, and d is the resulting dose distribution. The set of scenarios S contained up to 21 scenarios. Of the five different treatment plans created for each of the studied beam arrangements, one treatment plan was only made robust to setup errors of ±2 mm in every dimension, so S only contained seven scenarios: six setup error scenarios and the nominal scenario in which no errors occur. The remaining four treatment plans were made robust to range errors of 1%–4%, in increments of 1%, in addition to setup errors of ±2 mm in every dimension. Three different range error scenarios were included in the optimization: undershoot, nominal, and overshoot. In these cases, S therefore contained 21 scenarios: the aforementioned seven positional scenarios in each of the three range scenarios Target coverage was kept consistent between both beam arrangements, all levels of range uncertainty, and all scenarios, and clinical constraints kept the maximum dose within the target below 104% of the prescription dose in all cases. A potential trade-off between dose hotspots within the target and sparing of nearby OARs or healthy tissue therefore did not have to be considered.[33] The number of variables and constraints for the 0% range uncertainty robustness treatment plans of all 10 patients included in this study are shown in Table 1.

Setup and range uncertainty robustness were achieved through isocenter shifts and by uniform scaling of the Hounsfield unit (HU) values in the patient CT.[22,23,34–37] Undershoot and overshoot scenarios are defined as range error scenarios in which the HUs in the patient CT were scaled with a scaling factor > 1 and a scaling factor < 1, respectively. All target planning constraints and objectives were applied to all scenarios included in the optimization. Only a single clinical planning CT was available for every patient, so anatomical robustness was not implemented.[38–40]

TABLE 1 Numbers of variables and constraints for all patients

Patient #	# of variables ($\times 10^3$)	# of constraints ($\times 10^3$)
1	75.2	586.4
2	162.6	866.1
3	598.9	831.1
4	310.1	1113.3
5	355.3	894.6
6	394.0	492.1
7	492.8	655.4
8	596.7	1796.0
9	576.1	1060.3
10	697.3	1221.8

The number of variables and constraints for the 0% range uncertainty robustness treatment plan of the traditional beam arrangement for all 10 patients included in this study. Values for higher levels of range uncertainty robustness differ due to the increased number of scenarios. Objective functions included maximize minimum dose, maximize mean dose, minimize maximum dose, minimize mean dose, and minimize over-/underdose with respect to a specified threshold.

For each of the studied beam arrangements, the aforementioned steps yielded five different sets of fluences $\vec{x}$, which corresponded to range uncertainty robustness levels of 0%–4%. A dose distribution d_s was calculated for every range uncertainty robustness level and every scenario s:

$$d_s = D^s\vec{x} \quad (2)$$

This yielded seven dose distributions for treatment plans not robust to any range errors and 21 dose distributions for all other treatment plans. The intensity-modulated proton therapy (IMPT) approach was chosen for all optimizations, meaning that field-wise dose distributions were allowed to be non-uniform as long as the uniformity of the total dose distribution was preserved.[28]

2.4 | Monte Carlo simulations of dose and dose-averaged linear energy transfer (LET_d) distributions

To verify the accuracy of treatment planning system (TPS)-based results and the underlying pencil beam algorithm, Monte Carlo simulations were performed for the nominal scenario of the treatment plans only robust to setup errors of ±2 mm using the TOPAS Monte Carlo tool.[41] The TOPAS workflow only required the patient

CT and the relevant treatment plan as inputs. Brainstem NTCPs calculated using Monte Carlo simulation-based dose distributions were then compared to the corresponding TPS-based values. Dose-averaged linear energy transfer (LET_d) distributions were determined as well to provide additional information on the potential effects of the novel beam arrangements studied.

2.5 | Evaluation of dose distributions

A Python tool was created for the evaluation of all resulting dose distributions. Different target coverage metrics such as the percentage of the target volume receiving at least 95% of the prescription dose were determined to verify that target coverage was consistent for both beam arrangements, all range uncertainty levels, and all scenarios. Metrics including mean and maximum doses as well as NTCPs were determined for all potentially relevant OARs.

NTCPs were calculated using the Lyman-Kutcher-Burman (LKB) model, which relies on the following parameters[42]:

- **TD50**: tolerance dose at which an NTCP of 50% is observed
- ***n***: governs the NTCP's volume dependence
- ***m***: determines the slope of the dose-NTCP curve
- **Dose**: modeled as the entire OAR being irradiated with an effective dose, as suggested by Mohan et al.[43]

NTCPs were determined for all OARs within 1 cm of the target to assure that the novel beam arrangement did not inadvertently create a different trade-off between the NTCP for the brainstem and complication probabilities of other OARs. OARs further than 1 cm from the target were not considered relevant because they are expected to be largely unaffected by the investigated changes in range uncertainty. The presented results will limit themselves to the brainstem as the only OAR which was relevant in at least five cases.

The parameters used to calculate the brainstem NTCP with the endpoint of necrosis were $n = 0.16$, $m = 0.14$, and TD50 = 65 Gy(RBE). These parameter values may be conservative and may therefore overestimate the true NTCPs.[42,44] The healthy brain volume receiving a dose of at least 30 Gy(RBE) was determined as well because it has been linked to a range of impairments such as a reduction in the working memory.[45]

3 | RESULTS

3.1 | Results based on TPS dose calculations

For all patients, both beam arrangements, and all range uncertainty robustness levels, the brainstem NTCP in the nominal and the best-case and worst-case scenario is shown in Figure 2. Best-case and worst-case here refer to the scenario in which the relevant metric is lowest and highest, respectively. The novel beam arrangement was expected to be linked to a trade-off with regard to brainstem sparing: at low levels of range uncertainty robustness, the novel beam arrangement was expected to reduce the dose to the brainstem because the steeper dose fall-off at the distal beam edge was expected to allow for a more conformal dose distribution at the target-brainstem interface. At higher levels of range uncertainty, on the other hand, the novel beam arrangement was expected to deliver a higher dose to the brainstem than the traditional clinical beam arrangement, especially in the worst-case scenario, as greater use of the distal beam edge was expected to cause additional dose to be "pushed" into the brainstem. This trend was generally observed and can be seen especially clearly in the data for patients 7 to 10 in Figure 2.

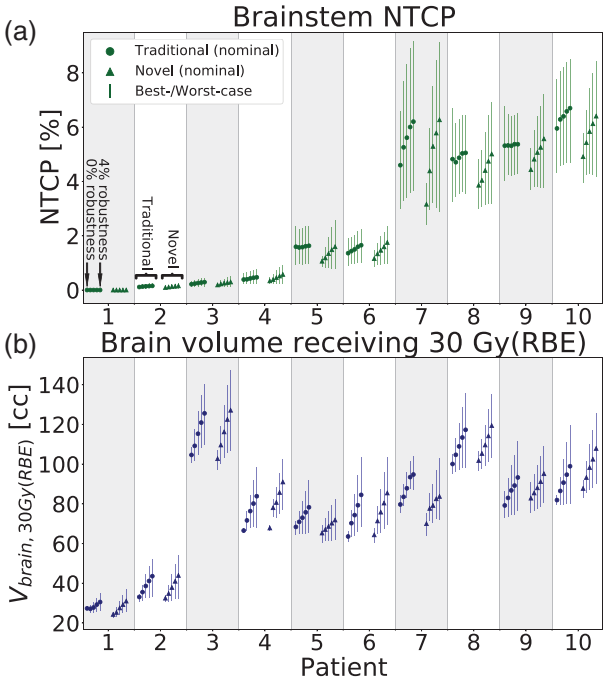

FIGURE 2 The (a) brainstem NTCP and (b) healthy brain volume receiving a dose of at least 30 Gy(RBE) for all patients, both beam arrangements, and all range uncertainty robustness levels. In every patient column, circles and triangles indicate the traditional clinical and the novel beam arrangement, respectively. Within a set of data points, range uncertainty robustness ranges from 0% on the left to 4% on the right. Data points indicate the values in the nominal scenario while error bars indicate the best-case and worst-case scenario for the relevant metric. In (a), differences in the results for different patients are explained by patient-specific factors such as prescription dose and target volume. The general healthy tissue dose was expected to be comparable for both beam arrangements, so no benefits were expected to be observed in (b)

The point at which novel beam arrangements become favorable—that is, maintain or reduce the brainstem NTCP compared to the traditional clinical beam

TABLE 2 Novel beam arrangement favorability as a function of range uncertainty

Range uncertainty (%)	Favorable novel beam arrangements [%]	
	Nominal scenario	Worst-case scenario
0	100	100
1	100	100
2	100	100
3	90	80
4	60	40

The percentage of favorable novel beam arrangements for all levels of range uncertainty robustness and the nominal and worst-case scenario. Favorability is defined as the novel beam arrangement maintaining or reducing the brainstem NTCP compared to the traditional clinical beam arrangement. All novel beam arrangements were favorable starting at a range uncertainty of 2%. Many novel beam arrangements, however, became favorable at a range uncertainty >2%.

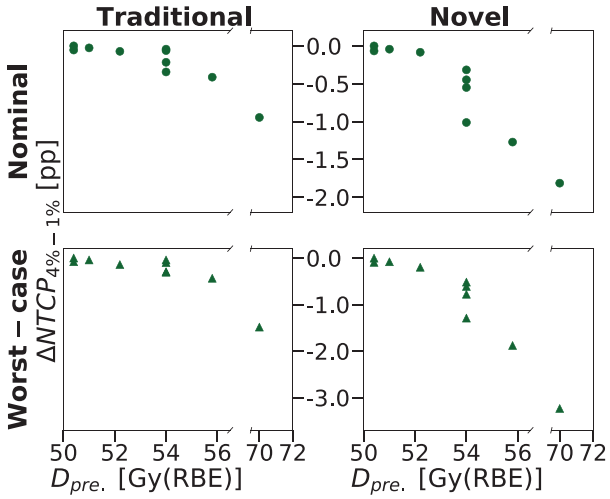

FIGURE 3 The brainstem NTCP decreases caused by a 4% to 1% range uncertainty reduction as a function of prescription dose D_{pre}. The left and right column concern the use of the traditional clinical beam arrangement and the novel beam arrangement, respectively, at a range uncertainty of 1%. The first and second row depict the data in the nominal and in the worst-case scenario. Every data point reflects one patient, and the data point with a prescription dose of 70 Gy(RBE) corresponds to a case in which a CTV with a prescription dose of 56 Gy(RBE) contained a sub-structure with a prescription dose of 70 Gy(RBE). Values correspond to the differences between the 4% and 1% data points shown in Figure 2. The unit pp refers to percentage points

arrangement—is essential, as it determines by how much the current range uncertainty would have to be reduced for novel beam arrangements to become viable and for the associated NTCP reductions to be achieved. For the nominal and the worst-case scenario, the percentage of cases for which the novel beam arrangement was favorable as a function of range uncertainty is shown in Table 2. Compared to the traditional clinical beam arrangement, the novel beam arrangement reduced the brainstem NTCP in all cases starting at a range uncertainty of 2%. However, in many cases, the novel beam arrangement became favorable at a range uncertainty >2%. The feasibility of some novel beam arrangements at a range uncertainty of 4% is largely explained by cases in which the brainstem NTCP remained near or at 0% at all levels of range uncertainty.

The current clinical range uncertainty margin is institution-dependent and ranges from 2.5% + 1.5 mm to 3.5% + 3 mm.[2,46] This work therefore approximates the clinical range uncertainty margin as 4%. In vivo range verification methods, on the other hand, already report millimeter accuracy.[19,20] A range uncertainty reduction to a level of 1% may therefore eventually be achievable.

When solely relying on the traditional clinical beam arrangement, a range uncertainty reduction from 4% to 1% decreased the brainstem NTCP by up to 0.9 percentage points in the nominal scenario and by up to 1.5 percentage points in the worst-case scenario. When taking the feasibility of novel beam arrangements at low levels of range uncertainty into account, however, a 4% to 1% range uncertainty reduction decreased the brainstem NTCP by up to 1.8 percentage points in the nominal scenario and by up to 3.2 percentage points in the worst-case scenario. The benefits of range uncertainty reductions generally increased with the prescription dose. For both beam arrangements, the brainstem NTCP decreases caused by a range uncertainty reduction from 4% to 1% as a function of prescription dose are shown in Figure 3.

Novel beam arrangements being linked to larger range uncertainty reduction benefits was attributable to the greater use of the sharper dose fall-off at the distal beam edge to conform the dose distribution to the brainstem. This is visualized in Figure 4, which depicts the nominal dose distributions of the 0% range uncertainty robustness treatment plan for patient 8 for both beam arrangements as well as the dose changes caused by increasing range uncertainty robustness from 0% to 4%. Despite comparable target coverage, the novel beam arrangement was able to deliver a lower dose to the brainstem when range uncertainty was low. At higher levels of range uncertainty, however, the novel beam arrangement caused additional dose to be "pushed" into the brainstem, while the traditional clinical treatment plan caused additional dose to be deposited along the target's boundary with the brainstem instead.

3.2 | Monte Carlo simulations to verify dose calculation accuracy

For all ten cases included in this study, the TPS- and Monte Carlo simulation-based brainstem NTCP for the nominal scenario of the treatment plan only robust to setup errors of ±2 mm is shown in Figure 5. Monte Carlo

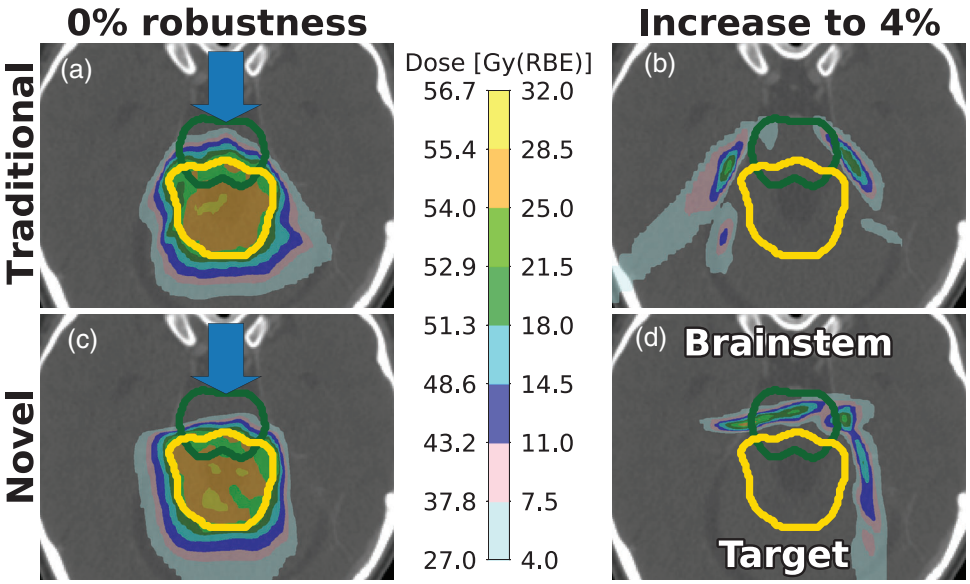

FIGURE 4 The dose distribution for the treatment plan only robust to setup errors of ±2 mm for the (a) traditional clinical and (b) novel beam arrangement and the dose changes caused by increasing range uncertainty robustness from 0% to 4% for the (c) traditional clinical and (d) novel beam arrangement for patient 8. All dose distributions concern the nominal scenario. Arrows emphasize the brainstem sparing achieved by the novel beam arrangement at low levels of range uncertainty. The green and yellow structure depicted are the brainstem and the CTV, respectively

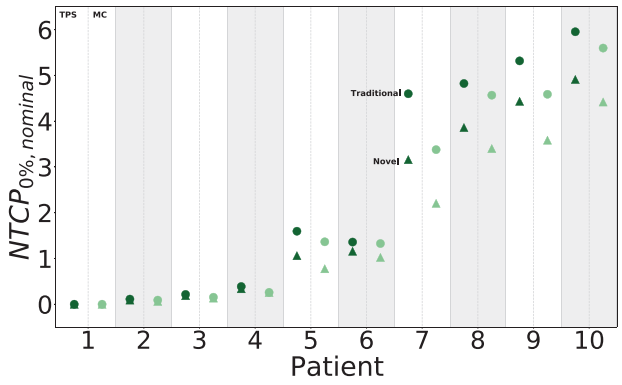

FIGURE 5 The brainstem NTCP with the endpoint of necrosis for all 10 patients included in this study. Circles and triangles indicate values for the traditional clinical and the novel beam arrangement, respectively. Within each patient column, data points on the left and right concern treatment planning system (TPS)- and Monte Carlo (MC) simulation-based dose calculations, respectively. All data points concern the nominal scenario of the treatment plan only robust to setup errors of ±2 mm

simulation-based dose distributions resulted in small differences in the absolute NTCP values as compared to TPS dose calculations, for both the traditional and novel beam arrangement. This was because more accurate modeling of multiple Coulomb scattering by Monte Carlo simulations resulted in slight differences in the end-of-range of the proton beams. However, the reduction of the NTCP achieved by the novel beam arrangements remained almost identical to the differences observed for TPS dose calculations.

4 | DISCUSSION

4.1 | Radiobiological effects at the end of range

As is done in clinical practice, dose calculations applied a relative biological effectiveness (RBE) value of 1.1 to account for the differences between photon and proton irradiation. Models in which the RBE is a function of parameters like dose and LET are being investigated.[47–49] However, RBE will depend on the specific endpoint that is considered, and variable RBE models are generally based on data for clonogenic cell survival and therefore more relevant for target structures than organs-at-risk, in addition to being associated with considerable uncertainties.[50,51]

For brainstem necrosis specifically, clinical studies of pediatric patients with central nervous system (CNS) malignancies, low-grade glioma, and posterior fossa tumors indicate that proton therapy is associated with lower or comparable toxicity rates than conventional photon treatments.[52–54] In addition, a study which included 111 medulloblastoma patients who received proton therapy and which focused on patients with clinical symptoms of CNS or brainstem injury observed higher LET values compared to the target but statistically not significant RBE differences in 8 out of 10 treatment change areas identified using magnetic resonance imaging (MRI).[55] The study also reported CNS and brainstem injury rates that were comparable to those associated with photon treatments.

TABLE 3 The mean dose-averaged linear energy transfer (LET_d) within the brainstem for all 10 cases

Patient #	LET_d [keV/μm]	
	Traditional	Novel
1	5.5	5.2
2	3.3	3.3
3	3.1	3.7
4	5.2	5.1
5	4.6	6.1
6	2.7	3.1
7	2.5	2.7
8	4.0	5.7
9	4.0	5.7
10	4.0	4.3

The mean dose-averaged linear energy transfer (LET_d) within the brainstem for all 10 cases included in this study. All values concern the nominal scenario of the treatment plan only robust to setup errors of $\pm$2 mm.

The potential effects of differences in LET between the traditional and novel beam arrangement have to be taken into account nonetheless. Table 3 contains the simulated mean LET_d within the brainstem for the nominal scenario of the treatment plan only robust to setup errors of $\pm$2 mm for all cases and both beam arrangements included in this study. Monte Carlo simulations showed that the novel beam arrangement led to an increase in the mean LET_d within the brainstem for some of the investigated cases.

Previous studies suggest a variable RBE-induced range uncertainty of approximately a few millimeters or <2%.[2,48,56] The novel beam arrangement, on the other hand, was favorable—that is, maintained or reduced brainstem NTCP in all cases and scenarios compared to the traditional clinical beam arrangement—at a range uncertainty of 2%, and became feasible at a range uncertainty >2% in most cases. The novel beam arrangement would therefore have remained beneficial when including the effects of variations in RBE, provided range uncertainties can be reduced to a sufficiently low level.

LET-based optimization could be applied to determine whether novel beam arrangements may be able to achieve comparable or lower LET_d in nearby OARs when LET is optimized in addition to dose.[47] This study applied the same (dose-based) planning constraints and objectives as the patients' original clinical treatment plans, so LET within the brainstem was not included in any of the optimizations. The observed differences in LET distributions between the two beam arrangements may therefore be able to be reduced if LET-based planning constraints and objectives are included in addition to conventional dose-based ones. Applying LET-based optimization may reduce the range uncertainty reduction benefits as quantified in this study but would also help mitigate the risk of potential LET effects. The variable RBE-induced range shift, which has been quantified previously for some cases, could likewise be taken into account during treatment planning, for example as a modifier applied to the proton beam range.[2,48,56]

The traditional beam arrangement generally exhibited lower mean LET_d within the brainstem than the novel beam arrangement, and range uncertainty reduction benefits for traditional beam arrangements have been quantified in this as well as previous studies.[22–24] However, range uncertainty reduction benefits associated with the novel beam arrangement as quantified in this study were twice as high or higher than the benefits associated with the traditional beam arrangement. Solely relying on the traditional beam arrangement may therefore prevent the potential benefits of range uncertainty reductions from being fully utilized.

Once novel beam arrangements have been investigated in greater detail and range uncertainties have been reduced to a sufficient level, a clinical study may be able to help determine the benefits of novel beam arrangements over traditional clinical ones. However, since brainstem necrosis is a severe side effect and treatment planning therefore takes care to keep brainstem necrosis rates low, such a study would have to be sufficiently large for potential differences between brainstem necrosis rates to be observed.

4.2 | Range uncertainty reductions necessary for novel beam arrangements to become favorable

At the current clinical range uncertainty, which is institution-dependent and which can be approximated as 4%, the novel beam arrangement was frequently unfavorable in terms of brainstem NTCP compared to the traditional clinical beam arrangement.[2,46] This trend was expected because the current reliance on the less steep dose fall-off at the lateral beam edge is motivated by improved OAR and healthy tissue sparing in a wide range of scenarios at higher levels of range uncertainty.

The level to which the current range margin would have to be reduced for novel beam arrangements to become favorable was 2% for both the nominal and worst-case scenario. Most novel beam arrangements became favorable at a range uncertainty >2%, and improvements in the favorability of novel beam arrangements were observed between all levels of range uncertainty. Smaller range uncertainty reductions were therefore also beneficial. The range uncertainty reduction necessary for novel beam arrangements to become favorable is expected to depend on factors such as treatment site and relevant OARs. In all cases, the novel beam arrangement was able to reduce the brainstem NTCP at low levels of range uncertainty without compromising the sparing of other OARs or healthy tissue.

The range of the TPS pencil beam algorithm was validated using Monte Carlo simulations. TPS-based NTCPs were generally slightly higher but in good agreement with NTCPs calculated based on Monte Carlo simulations. At a low level of range uncertainty, the novel beam arrangement remained beneficial in terms of brainstem NTCP even when dose calculations were Monte Carlo simulation based. Although absolute NTCPs varied, the magnitude of this benefit was consistent with the results of TPS dose calculations.

4.3 | Candidate cases especially benefitting from range uncertainty reductions

The benefits of range uncertainty reductions increased with prescription dose and, to a lesser extent, target volume. The former was particularly relevant because CTV prescription doses, which ranged from 50.4 Gy(RBE) to 56 Gy(RBE), were low relative to NTCP model parameters such as the tolerance dose of TD50 = 65 Gy(RBE).[42,44] Even a prescription dose difference of a few Gy(RBE) therefore frequently affected the magnitude of the observed NTCP reductions markedly. The relationship between prescription dose and brainstem sparing is in line with what we observed in our previous work, which focused solely on skull base cases.[24] The relevance of the prescription dose is expected to vary depending on factors such as the OAR in question and the chosen NTCP model parameters.

The relationship between target size and NTCP reduction magnitude was attributable to the comparatively large volume of the brainstem, which was usually in the dozens of cc. This is because comparatively low prescription doses led to a larger part of the OAR having to receive a considerable dose for NTCP changes to be observed. However, target size is not expected to have a crucial effect for all OARs. Our previous study suggests that for smaller organs at risk such as the optic chiasm, proximity to the target plays a greater role.[24] This is because such organs are generally small enough for a considerable portion of the OAR to receive a significant dose whenever the OAR in question is in close proximity to the target.

4.4 | The relative importance of considering novel beam arrangements

It has been suggested that the benefits of range uncertainty reductions may be much smaller than the OAR dose reductions achieved by reducing setup uncertainties.[22,23] As this study focused on the interplay between novel beam arrangements and range uncertainty reductions specifically, our results do not allow us to draw any conclusions regarding this exact point. Our results do, however, indicate that only considering the direct effects of range uncertainty reductions may drastically underestimate the total benefits of reducing range uncertainties. Range uncertainty reduction benefits achieved through novel beam arrangements exceeded the benefits when only relying on the traditional clinical beam arrangement in all patients, in some cases by a factor of 2 or more. Future studies should therefore include indirect benefits of range uncertainty reductions such as the feasibility of novel beam arrangements, as not doing so may underestimate the benefits of range uncertainty reductions markedly.

4.5 | LKB model parameters

The parameters used in the LKB model underlying the brainstem NTCP calculations may be conservative.[42,44] If potentially less conservative parameters—for example, a higher TD50 value—were available and had been applied, calculated brainstem NTCPs would have been lower. Potentially reducing the risk of brainstem necrosis is relevant because of its severity, but it is also an uncommon side effect, with necrosis rates of 0.7% and 1.1% and a 5-year brainstem injury rate <2% having been reported.[52,53,57]

Range uncertainty reduction benefits could have been quantified in terms of dose rather than NTCP. This would have made results independent of uncertainties in LKB model parameters. However, doing so would have come with its own shortfalls. A 5 Gy(RBE) reduction in the maximum dose to the brainstem, for example, may be more relevant for higher initial maximum brainstem doses. Results were represented in terms of NTCP rather than dose because the LKB model already takes such factors into account, in addition to also considering aspects such as volume-dependence.

4.6 | Effects of methodological differences like beam angle optimization and the inclusion of additional uncertainties

For this study, novel beam arrangements were chosen manually. However, beam angle optimization approaches are also being investigated.[58,59] While novel beam arrangements were favorable at low levels of range uncertainty despite manual beam angle selection, beam direction optimization may have been able to determine even more beneficial beam arrangements compared to the traditional clinical beam arrangement. The quantified benefits of novel beam arrangements may therefore have been greater if beam angle optimization rather than manual beam angle selection had been applied.

The traditional beam arrangement was defined as the clinical beam arrangement with which a given patient had been treated. We therefore did not consider it necessary to define alternative traditional beam arrangements. However, if beam angle optimization was applied to determine novel beam arrangements, traditional beam arrangements should be determined in the same way to assure a fair comparison.

As mentioned in Section 2.3, anatomical robustness was not included in this study because only a single planning CT was available for every patient.[39,40] Including such additional uncertainties in the optimizations (or other methodological differences related to the optimizations) may affect results. As with beam angle optimization, any changes in methodology should be consistent for all beam arrangements to assure that the comparison is fair.

5 | CONCLUSION

We have investigated the benefits of range uncertainty reductions in 10 brain cancer and skull base cases treated with IMPT, with a focus on novel beam arrangements made feasible by reductions in proton range uncertainties. The benefit of novel beam arrangements and range uncertainty reductions was quantified in terms of the associated decrease in brainstem NTCP with the endpoint of brainstem necrosis, a rare but severe side effect. When only considering the traditional clinical beam arrangement, a range uncertainty reduction from the current margin of approximately 4% to a potentially achievable level of 1% decreased the brainstem NTCP by up to 0.9 percentage points in the nominal scenario and by up to 1.5 percentage points in the worst-case scenario. When taking into account the feasibility of novel beam arrangements at lower levels of range uncertainty, however, a 4% to 1% range uncertainty reduction decreased the brainstem NTCP by up to 1.8 percentage points in the nominal scenario and by up to 3.2 percentage points in the worst-case scenario. The novel beam arrangement became favorable in terms of brainstem NTCP at a range uncertainty of 2%. In most cases, the novel beam arrangement became favorable at a range uncertainty >2%. This suggests that the novel beam arrangement would remain beneficial even if RBE-induced range uncertainties are considered, provided range uncertainties can be reduced to a sufficiently low level. Future studies should nonetheless optimize LET in addition to dose to investigate whether the novel beam arrangement may be able to achieve LET benefits similar to the advantages in NTCP reduction quantified in this study.

The NTCP reductions achieved by novel beam arrangement exceeded the direct benefits of range uncertainty reductions, by as much as a factor of 2 or more in some cases. Considering indirect benefits of range uncertainty reductions, such as the feasibility of novel beam arrangements at lower levels of range uncertainty, may therefore be crucial in determining the full benefits of reducing proton range uncertainties.

ACKNOWLEDGMENTS

We thank Bram L. Gorissen for his help with the robust optimization workflow underlying this work, and Aimee McNamara, Jungwook Shin, and Hoyeon Lee for their support with the TOPAS portion of this project. This work was supported in part by the Federal Share of program income earned by Massachusetts General Hospital on C06-CA059267, Proton Therapy Research and Treatment Center, and by the National Cancer Institute grant R01-CA229178, Fast Individualized Delivery Adaptation in Proton Therapy. S.T. was also supported by a scholarship awarded by the Monika Kutzner Foundation, a German foundation dedicated to supporting cancer research.

Open Access funding enabled and organized by Projekt DEAL.

CONFLICT OF INTEREST

The authors declare no conflict of interest.

DATA AVAILABILITY STATEMENT

The data that support the findings of this study are available from the corresponding author upon reasonable request.

REFERENCES

1. Wilson R. Radiological use of fast protons. *Radiology*. 1946;47(5):487-491.
2. Paganetti H. Range uncertainties in proton therapy and Monte Carlo simulations. *Phys Med Biol*. 2012;57(11):R99-R117.
3. Knopf A, Lomax A. In vivo proton range verification: a review. *Phys Med Biol*. 2013;58(15):R131-160.
4. Fredriksson A, Bokrantz R. A critical evaluation of worst case optimization methods for robust intensity-modulated proton therapy planning. *Med Phys*. 2014;41(8):081701.
5. Unkelbach J, Alber M, Bangert M, et al. Robust radiotherapy planning. *Phys Med Biol*. 2018;63(22):22TR02.
6. Bär E, Lalonde A, Royle G, Lu H-M, Bouchard H. The potential of dual-energy CT to reduce proton beam range uncertainties. *Med Phys*. 2017;44(6):2332-2344.
7. Wohlfahrt P, Möhler C, Hietschold V, et al. Clinical implementation of dual-energy CT for proton treatment planning on pseudo-monoenergetic CT scans. *Int J Radiat Oncol Biol Phys*. 2017;97(2):427-434.
8. Taasti V, Muren L, Jensen K, et al. Comparison of single and dual energy CT for stopping power determination in proton therapy of head and neck cancer. *phiRO*. 2018;6:14-19.
9. Sadrozinski H, Geoghegan T, Harvey E, et al. Operation of the preclinical head scanner for proton CT. *Nucl Instrum Methods Phys Res A*. 2016;831:394-399.
10. Cassetta R, Piersimoni P, Riboldi M, et al. Accuracy of low-dose proton CT image registration for pretreatment alignment verification in reference to planning proton CT. *J Appl Clin Med Phys*. 2019;20(4):83-90.

11. Tanaka S, Nishio T, Tsuneda M, Matsushita K, Kabuki S, Uesaka M. Improved proton CT imaging using a bismuth germanium oxide scintillator. *Phys Med Biol*. 2018;63(3):035030.
12. Dedes G, Dickmann J, Niepel K, et al. Experimental comparison of proton CT and dual energy x-ray CT for relative stopping power estimation in proton therapy. *Phys Med Biol*. 2019;64(16):165002.
13. Parodi K, Paganetti H, Shih H, et al. Patient study of in vivo verification of beam delivery and range, using positron emission tomography and computed tomography imaging after proton therapy. *Int J Radiat Oncol Biol Phys*. 2007;68(3):920-934.
14. Knopf A, Parodi K, Paganetti H, et al. Accuracy of proton beam range verification using post-treatment positron emission tomography/computed tomography as function of treatment site. *Int J Radiat Oncol Biol Phys*. 2011;79(1):297-304.
15. Min C, Zhu X, Winey B, et al. In vivo treatment verification using in-room PET in proton radiation therapy: first clinical trials and evaluation of short-length scan. *Int J Radiat Oncol Biol Phys*. 2012;84(3):S53-S54.
16. Grogg K, Zhu X, Shih H, Alpert N, El Fakhri G. Proton range verification with PET imaging in brain and head and neck cancers. *J Nucl Med*. 2018;59(1S):658.
17. Ferrero F, Fiorina E, Morrocchi M, et al. Online proton therapy monitoring: clinical test of a silicon-photodetector-based in-beam PET. *Sci Rep*. 2018;8(1):4100.
18. Min C, Kim C. Prompt gamma measurements for locating the dose falloff region in the proton therapy. *Appl Phys Lett*. 2006;89(18):183517.
19. Richter C, Pausch G, Barczyk S, et al. First clinical application of a prompt gamma based in vivo proton range verification system. *Radiother Oncol*. 2016;118(2):232-237.
20. Hueso-Gonzalez F, Rabe M, Ruggieri T, Bortfeld T, Verburg J. A full-scale clinical prototype for proton range verification using prompt gamma-ray spectroscopy. *Phys Med Biol*. 2018;63(18):185019.
21. Draeger E, Mackin D, Peterson S, et al. 3D prompt gamma imaging for proton beam range verification. *Phys Med Biol*. 2018;63(3):035019.
22. Van de Water S, van Dam I, Schaart D, Al-Mamgani A, Heijmen B, Hoogeman M. The price of robustness; impact of worst-case optimization on organ-at-risk dose and complication probability in intensity-modulated proton therapy for orpharyngeal cancer patients. *Radiother Oncol*. 2016;120(1):56-62.
23. Wagenaar D, Kierkels R, Van der Schaaf A, et al. Head and neck IMPT probabilistic dose accumulation: feasibility of a 2 mm setup uncertainty setting. *Radiother Oncol*. 2021;154:45-52.
24. Tattenberg S, Madden T, Gorissen, B L, Bortfeld T, Parodi K, Verburg J. Proton range uncertainty reduction benefits for skull base tumors in terms of normal tissue complication probability (NTCP) and healthy tissue doses. *Med Phys*. 2021;48(9):5356-5366.
25. Deasy J, Shepard D, Mackie T. Distal edge tracking: a proposed delivery method for conformal proton therapy using intensity modulation: *Proceedings XIIth ICCR*, Salt Lake City; 1997.
26. Trofimov A, Bortfeld T. Optimization of beam parameters and treatment planning for intensity modulated proton therapy. *Technol Cancer Res Treat*. 2003;2(5):437-444.
27. Liu W, Li Y, Li X, Cao W, Zhang X. Influence of robust optimization in intensity-modulated proton therapy with different dose delivery techniques. *Med Phys*. 2012;39(6):3089-3101.
28. McGowan S, Burnet N, Lomax A. Treatment planning optimization in proton therapy. *Br J Radiol*. 2013;86(1021):20120288.
29. Kooy H, Clasie B, Lu, H-M, et al. A case study in proton pencil-beam scanning delivery. *Int J Radiat Oncol Biol Phys*. 2010;76(2):624-630.
30. Hong L, Goitein M, Bucciolini M, Comiskey R, Gottschalk B, Rosenthal S, Serago C, Urie M. A pencil beam algorithm for proton dose calculations. *Phys Med Biol*. 1996;41(8):1305-1330.
31. Gorissen B.L. Interior point methods can exploit structure of convex piecewise linear functions with application in radiation therapy. *SIOPT*. 2022;32(1):256-275.
32. Gondzio J. Interior point methods 25 years later. *Eur J Oper Res*. 2011;218(3):587-601.
33. Petit S, Seco J, Kooy H. Increasing maximum tumor dose to manage range uncertainties in IMPT treatment planning. *Phys Med Biol*. 2013;58(20):7329-7341.
34. Fredriksson A, Forsgren A, Hårdemark B. Minimax optimization for handling range and setup uncertainties in proton therapy. *Med Phys*. 2011;38(3):1672-1684.
35. Liu W, Zhang X, Li Y, Mohan R. Robust optimization of intensity modulated proton therapy. *Med Phys*. 2012;39(2):1079-1091.
36. Liu W, Frank S, Li X, Li Y, Zhu R, Mohan R. PTV-based IMPT optimization incorporating planning risk volumes vs robust optimization. *Med Phys*. 2013;40(2):021709.
37. Liu W, Frank S, Li X, et al. Effectiveness of robust optimization in intensity-modulated proton therapy planning for head and neck cancers. *Med Phys*. 2013;40(5):051711.
38. Van de Water S, Albertini F, Weber D, Heijmen B, Hoogeman M, Lomax A. Anatomical robust optimization to account for nasal cavity filling variation during intensity-modulated proton therapy: a comparison with conventional and adaptive planning strategies. *Phys Med Biol*. 2018;63(2):025020.
39. Yang Z, Zhang X, Wang X, , et al. Multiple-CT optimization: an adaptive optimization method to account for anatomical changes in intensity-modulated proton therapy for head and neck cancers. *Radiother Oncol*. 2020;142:124-132.
40. Cubillos-Mesías M, Troost E, Lohaus F, et al. Quantification of plan robustness against different uncertainty sources for classical and anatomical robust optimized treatment plans in head and neck cancer proton therapy. *Br J Radiol*. 2020;93(1107):20190573.
41. Perl J, Shin J, Schümann J, Faddegon B, Paganetti H. TOPAS: an innovative proton Monte Carlo platform for research and clinical applications. *Med Phys*. 2012;39(11):6818-6837.
42. Burman C, Kutcher G, Emami B, Goitein M. Fitting of normal tissue tolerance data to an analytic function. *Int J Radiat Oncol Biol Phys*. 1991;21(1):123-135.
43. Mohan R, Mageras G, Baldwin B, et al. Clinically relevant optimization of 3-D conformal treatments. *Med Phys*. 1992;19(4):933-944.
44. Mayo C, Yorke E, Merchant T. Radiation associated brainstem injury. *Int J Radiat Oncol Biol Phys*. 2010;76(suppl 3):S36-S41.
45. Zureick A, Pulsifer M, Niemierko A, et al. Elevated proton radiation therapy dose to left temporal lobe or whole-brain correlates with decline in full-scale IQ components for pediatric CNS tumor survivors. *Int J Radiat Oncol Biol Phys*. 2016;96(2):S120.
46. Hahn C, Eulitz J, Peters N, et al. Impact of range uncertainty on clinical distributions of linear energy transfer and biological effectiveness in proton therapy. *Med Phys*. 2020;47(12):6151-6162.
47. Giantsoudi D, Grassberger C, Craft D, Niemierko A, Trofimov A, Paganetti H. Linear energy transfer-guided optimization in intensity modulated proton therapy: feasibility study and clinical potential. *Int J Radiat Oncol Biol Phys*. 2013;87(1):216-222.
48. Giovannini G, Böhlen T, Cabal G, et al. Variable RBE in proton therapy: comparison of different model predictions and their influence on clinical-like scenarios. *Radiat Oncol*. 2016;11(1):68.
49. McNamara A, Schuemann J, Paganetti H. A phenomenological relative biological effectiveness (RBE) model for proton therapy based on all published in vitro cell survival data. *Phys Med Biol*. 2015;60(21):8399-8416.
50. Paganetti H. Relative biological effectiveness (RBE) values for proton beam therapy. Variations as a function of biological endpoint, dose, and linear energy transfer. *Phys Med Biol*. 2014;59(22):R419-472.

51. Paganetti H. Mechanisms and review of clinical evidence of variations in relative biological effectiveness in proton therapy. *Int J Radiat Oncol Biol Phys*. 2022;112(1):222-236.
52. Vogel J, Grewal A, O'Reilly S, et al. Risk of brainstem necrosis in pediatric patients with central nervous system malignancies after pencil beam scanning proton therapy. *Acta Oncol*. 2019;58(12):1752-1756.
53. Indelicato D J, Rotondo R L, Uezono H, et al. Outcomes following proton therapy for pediatric low-grade Glioma. *Int J Radiat Oncol Biol Phys*. 2019;104(1):149-156.
54. Haas-Kogan D, Indelicato D, Paganetti H, et al. NCI workshop on proton therapy for children: considerations regarding brainstem injury. *Int J Radiat Oncol Biol Phys*. 2018;101(1):152-168.
55. Giantsoudi D, Sethi R V, Yeap B Y, et al. Incidence of CNS injury for a cohort of 111 patients treated with proton therapy for medulloblastoma: LET and RBE associations for areas of Injury. *Int J Radiat Oncol Biol Phys*. 2016;95(1):287-296.
56. Carabe A, Moteabbed M, Depauw N, Schuemann J, Paganetti H. Range uncertainty in proton therapy due to variable biological effectiveness. *Phys Med Biol*. 2012;57(5):1159-1172.
57. Gentile M S, Yeap B Y, Paganetti H, et al. Brainstem injury in pediatric patients with posterior fossa tumors treated with proton beam therapy and associated dosimetric factors. *Int J Radiat Oncol Biol Phys*. 2018;100(3):719-729.
58. Gu W, Neph R, Ruan D, Zou W, Dong L, Sheng K. Robust beam orientation optimization for intensity-modulated proton therapy. *Med Phys*. 2019;46(8):3356-3370.
59. Taasti V, Hong L, Shim J, Deasy J, Zarepisheh M. Automating proton treatment planning with beam angle selection using Bayesian optimization. *Med Phys*. 2020;47(8):3286-3296.

How to cite this article: Tattenberg S, Madden TM, Bortfeld T, Parodi K, Verburg J. Range uncertainty reductions in proton therapy may lead to the feasibility of novel beam arrangements which improve organ-at-risk sparing. *Med Phys*. 2022;49:4693-4704. https://doi.org/10.1002/mp.15644